

Experimental Determination of Scan-truncation Losses from Low-temperature (16 K) Single-crystal X-ray Measurements*

Riccardo Destro

Dipartimento di Chimica Fisica ed Elettrochimica, e Centro CNR,
Università di Milano, Via Golgi 19, Milano 20133, Italy.

Abstract

Model intensity profiles have been obtained for biscarbonyl[14]annulene by convoluting the Mo K α spectral distribution with two functions derived from experimental measurements at 16(1) K, up to $2\theta_{\text{Mo}} = 110^\circ$, of a spherical crystal mounted on a four-circle diffractometer equipped with the Samson low-temperature apparatus. The process includes accurate measurement of the inherent background, treatment of the profiles by numerical Fourier methods, and least-squares fitting. Owing to the instrumental configuration of the diffractometer used in this investigation, the first step of the process has required a careful determination of the χ dependence of the background, besides the usual 2θ dependence. Truncation losses for the crystal under study, evaluated for several scan ranges, are far larger than usually assumed or predicted.

1. Introduction

The solution to the problem of deducing an accurate and complete structural model from X-ray diffraction measurements alone requires high-quality data. In particular, if valence-electron distributions or atom-libration patterns are to be studied, high-angle data extending well beyond the Cu sphere (and possibly collected at low temperature) are almost mandatory in order for the 'thermal parameters' U_{ij} and the scale factor to be accurately assigned. However, high-angle intensity measurements from scanning diffractometers carry a certain loss in the measured integrated intensity due to the finite range of the scan. Since the amount of this loss depends on the scattering angle, the U_{ij} and the scale factor derived from data not corrected for scan-truncation losses are affected by systematic errors.

Denne (1977) has proposed an approximate evaluation of the corrections, but his approach to the problem seems somewhat inadequate when common data-collection techniques are employed. More recently, an empirical method for the evaluation of scan-truncation losses in single-crystal X-ray diffractometry has been suggested by Destro and Marsh (1987; hereinafter DM). These authors showed that an excellent model for ω - 2θ scan profiles of single-crystal intensities can be obtained by convoluting the spectral dispersion, calculated on the basis of theoretical components, with two functions derived from experimental measurements, the 'basic profile' and an angle-dependent function called the 'aberration function'. The basic profile is

* Paper presented at the International Symposium on Accuracy in Structure Factor Measurement, held at Warburton, Australia, 23-26 August 1987.

merely a low-angle ($2\theta < 10^\circ$) intensity profile, and its convolution with the spectral dispersion yields the *idealised* synthetic profile at any desired 2θ value. The unfolding of the latter from an experimental profile measured at the same 2θ angle gives the corresponding aberration function, whose essential features are found to be the same for *different* reflections of similar 2θ value. Once the average aberration function for a given 2θ range is calculated, a model profile can be obtained and the losses due to truncation evaluated for any desired scan range.

Because of the entirely empirical nature of the method, different values for the truncation corrections are to be expected from the treatment of data measured on different crystals and/or with different instrumental arrangements. Indeed, DM found analogous but not identical results for spherical crystals of l-alanine and citrinin, whose intensity profiles had been measured on the same diffractometer but with some instrumental differences. The present paper reports the results of the truncation analysis of a third crystal, whose intensity measurements have been carried out on a different diffractometer.

2. Experimental

All measurements were made on a crystal of biscarbonyl[14]annulene (BCA), ground to a sphere of radius 0.17 mm and mounted on the tip of a Pyrex glass fibre 0.15 mm in diameter. At the temperature of profile measurements [16(1) K], crystallographic data are: $a = 9.047(1)$ Å, $b = 12.667(2)$ Å, $c = 9.649(1)$ Å, $\beta = 94.34(1)^\circ$, $V = 1102.6(2)$ Å³; monoclinic, space group $P2_1/n$; $Z = 4$ (for a comparison with the room temperature values see Destro and Simonetta 1977). Data were collected in the ω - 2θ scan mode on a Syntex-Nicolet $P\bar{1}$ four-circle diffractometer equipped with a Samson low-temperature apparatus (Samson *et al.* 1980), where the sample crystal is enclosed in an evacuated ($P < 2 \times 10^{-5}$ Pa), nearly isothermal cavity. The diameter of the pinhole in the incident beam collimator was 1.4 mm, the thickness of the graphite monochromator crystal was about 0.8 mm, and the circular receiving aperture of the detector had a diameter of 2.5 mm. The diffractometer was equipped with a normal-focus Mo-target Philips X-ray tube, type PW2245/20, and the Iso-Debyelex 2002 generator operated at 50 kV and 30 mA. The monochromator was set at the configuration corresponding to $\epsilon = 90^\circ$ (Arndt and Willis 1966), that is, in the perpendicular geometry. The temperature was continuously measured and controlled by a Lake Shore DRC-80C instrument, equipped with a DT-500 DRC silicon-diode sensor.

Two sets of data with different scan ranges were collected, both up to $2\theta = 110^\circ$: one, with narrower scan range, to be used for subsequent refinement of positional and thermal parameters of BCA; the other, with larger scan range, for the study of truncation losses. The first dataset was collected with 2θ scan range $(2.5 + S)^\circ$, where S is the $K\alpha_1$ - $K\alpha_2$ splitting for Mo radiation; the scan rate was variable from 2.0 to 8.0° min⁻¹, and $t(B)/t(S)$ was 0.8 [where $t(B)$ is the time for background measurements at both ends of the scan range, each for a time equal to $\frac{1}{2}t(B)$, and $t(S)$ is the scan time]. In the range $0 < 2\theta < 55^\circ$ two full quadrants ($\pm h, k, l$ and $\pm h, -k, l$) were measured, one at the beginning and the other at the end of data collection, which lasted several weeks. In the $55^\circ < 2\theta < 110^\circ$ region only reflections whose intensities were > 10 c.p.s. (counts per second) in the prescan survey were collected and stored for subsequent use. Intensity and orientation stability of the

crystal were checked by repeated measurements of cell dimensions as well as by periodic monitoring of three standard reflections. Set 1 consisted of about 12000 measurements.

The second set, collected with an enlarged 2θ scan range ($3.4 + S$)°, included only relatively strong intensities, 20 to 40 within each of the eleven 10° intervals of 2θ . Some of them were collected several times, for a total of 649 profile measurements. For set 2, the scan rate varied from 0.5 to 1.0° min⁻¹, and $t(B)/t(S)$ was 0.5.

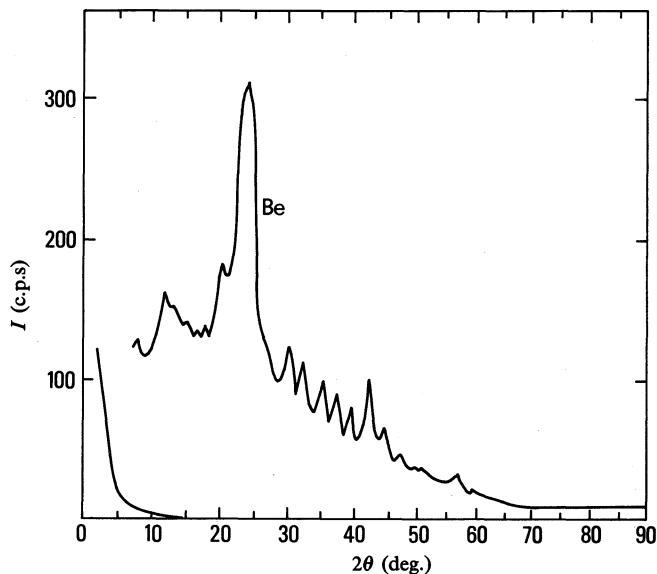


Fig. 1. Instrumental background of the Samson apparatus used in this work (lower curve) compared with that of beryllium-walled liquid-helium cryostats (upper curve, taken from Albertsson *et al.* 1979).

3. Background Measurement

In order to obtain a reliable evaluation of the truncation losses an accurate measurement of the inherent background must be performed. In this regard, it is worth while to compare the instrumental background of the Samson low-temperature chamber with that of previously described beryllium-walled liquid-helium cryostats (Coppens *et al.* 1974; Albertsson *et al.* 1979), where extensive scattering occurs from the Be walls. Fig. 1 shows the dramatic difference between the two types of instruments, and confirms that the aluminised Kapton foils used as windows in the Samson apparatus do not add an appreciable contribution to the air scattering. Hence, no special modifications in data-collection and data-processing software are required.

As in the case of the first application of the method to l-alanine and citrinin data, it is assumed that the effects of thermal diffuse scattering can be accounted for, at the temperature of intensity profiles measurements (16 K), by simply subtracting the inherent background from each of the 96 steps of a given profile. Under this assumption, DM have shown that the inherent background can be evaluated by making measurements either at points far distant from any reciprocal-lattice point or by merely averaging the background counts made on both sides of the weak

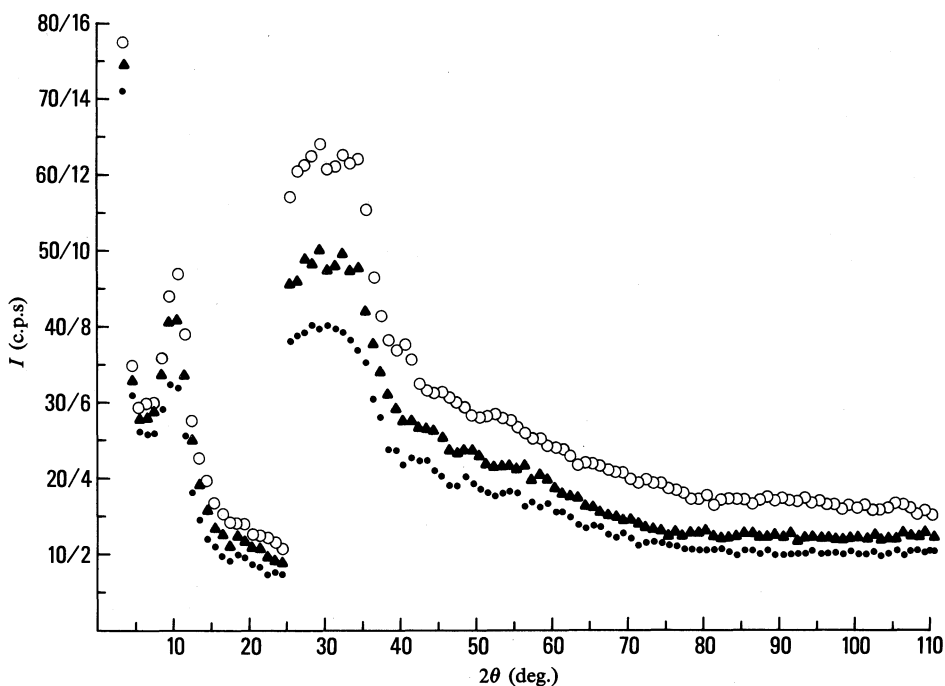


Fig. 2. The χ dependence of the contribution to the background due to the scattering of the glass fibre supporting the crystal at 16 K. Three average distributions measured at different χ values are shown: solid circles, $\chi < 10^\circ$; triangles, $30^\circ < \chi < 40^\circ$; and open circles, $\chi > 80^\circ$. Each point is the average of at least four measurements, each for a time of 60 to 180 s. Values for points at $2\theta < 25^\circ$ are on the larger ordinate scale (0–80 c.p.s.) and those at $2\theta > 25^\circ$ on the smaller scale (0–16 c.p.s.).

reflections. In the present case only the first procedure has been followed, since set 1 comprised too few weak reflections with $2\theta > 55^\circ$.

In contrast with the simple 2θ -dependence of the background of l-alanine and citrinin, for BCA a χ dependence was also to be expected, since the arrangement of the monochromator was such as to yield a monochromated beam with vertical dimension of about 1.0 mm (i.e. less than the diameter of the collimator pinhole), thus giving rise to an approximately elliptical shape for the incident beam itself. While this elliptical beam has no effect on the background due to the sample spherical crystal—if correctly centred on the goniometer—it affects significantly the portion of the background due to the glass fibre, the maximum contribution occurring at $\chi = 90^\circ$, where the fibre is parallel to the longest axis of the ellipse. To quantify and eventually parametrise this χ dependence, a glass fibre of the same dimensions as that supporting the crystal was mounted on the diffractometer, a similar amount of epoxy glue was added on top, and the height adjusted to reproduce the experimental conditions of data collection. At 16 K more than 6000 measurements were made, each for a time of 60 to 180 s, varying the χ value from 5° to 85° at steps of $\sim 10^\circ$, in the full 2θ range of sets 1 and 2 (0 to 110°). A portion of the results is shown in Fig. 2, where three background distributions are reported; the solid circles refer to the χ range 0 to 10° , the triangles to the range $30^\circ < \chi < 40^\circ$, and the open circles were obtained from the fibre set at $\chi > 80^\circ$.

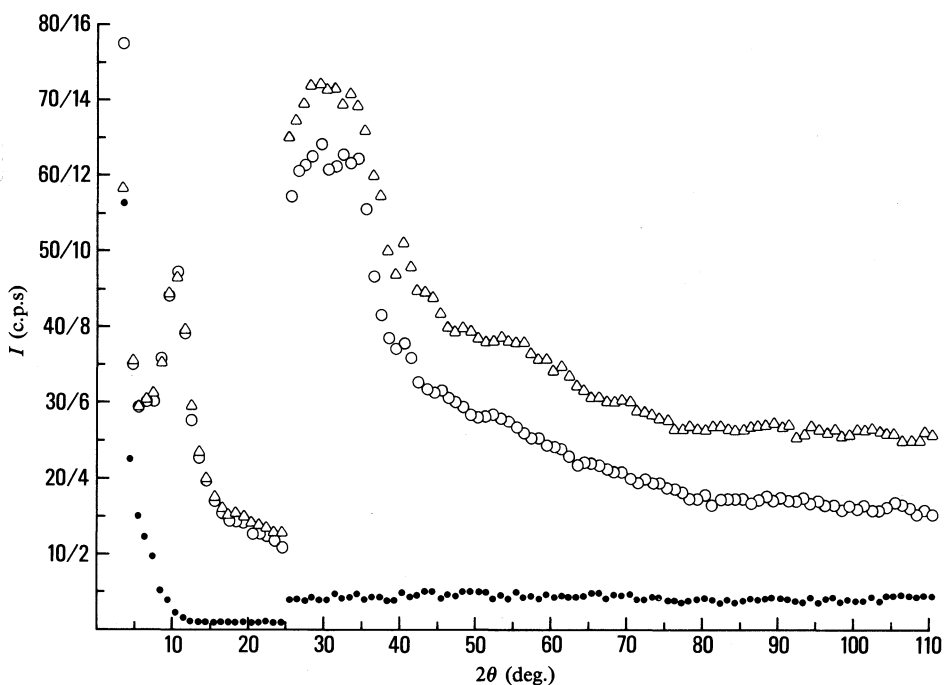


Fig. 3. Background distribution for BCA at 16 K for $\chi > 80^\circ$: triangles are the average distribution of the background derived from 1485 measurements, each for 60 to 180 s, at points far distant from reciprocal lattice points; open circles are the contribution to the background due to the scattering from air and specimen support (no crystal); and solid circles are the instrumental background (air and Kapton scattering, electronic noise, etc.). The ordinate scale is the same as in Fig. 2.

The same procedure was then repeated with the BCA crystal mounted, for a total of 4080 measurements, to assess which portion of the total background was due to the χ -independent contributors such as the crystal, the vacuum chamber, and the electronic noise, and which to the glass fibre. Fig. 3 shows the relevance of the scattering of the specimen support to the total background, a finding that confirms the results previously obtained by DM for l-alanine and citrinin. As expected, owing to the higher tube current and voltage employed for BCA, the backgrounds here are uniformly higher than those of the other two spherical crystals, but never exceed, at high 2θ angles, the value of 6 c.p.s., even when the contribution of the glass fibre is the largest (see Fig. 3).

4. Application of the Method

As described in greater detail by DM, each of the 649 profiles underwent a treatment comprising (i) replacement of the first and last of the 96 profile steps by the lengthier measurements of the apparent background; (ii) removal from each of the 96 steps of the 'true' background and normalisation of the total net intensity to a value of 10000; and (iii) smoothing by numerical Fourier methods to eliminate most of the statistical variations. The resulting smoothed profiles are called I_{exp} . By folding the basic profile (reflection $\bar{1}01$, $2\theta = 5.94^\circ$, $\text{FWHM} = 0.30^\circ$) with the appropriate spectral distribution of Mo $K\alpha$ radiation, the corresponding 649 *idealised*

(aberration-free) profiles $I_{b\lambda}$ were obtained, and the subsequent deconvolution of each pair of I_{exp} and $I_{b\lambda}$ yielded the Fourier transforms of the aberration functions. A weighted average of the latter—including all reflections measured within each of the eleven 10° intervals of the full 2θ scan range—gave the mean transform of the aberration function for each interval, and the corresponding non-idealised synthetic profiles could be computed.

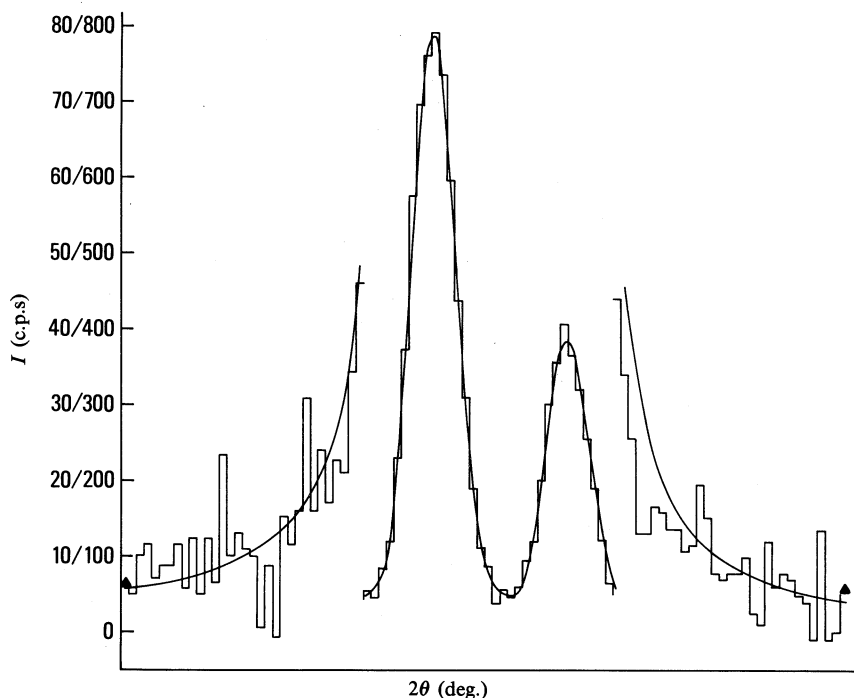


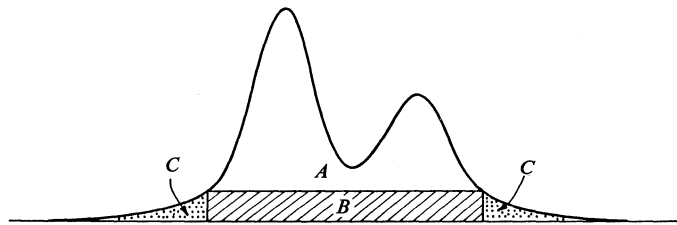
Fig. 4. Final synthetic profile for BCA at $2\theta = 95.0^\circ$ (continuous curve) superimposed on the background-free non-smoothed experimental profile (histogram) of reflection $-16,0,12$, measured at $2\theta = 95.59^\circ$. For the latter, the first and last of the 96 steps, marked by triangles, have been replaced by the more reliable values derived from the lengthier measurements of the *apparent* background.

Since numerical Fourier methods, as applied in the DM procedure, necessarily generate an oscillating behaviour in the region of the tails, that is in the region where a uniformly decreasing shape is required for a proper evaluation of the truncation errors, a further smoothing has to be performed on the synthetic non-idealised profiles to obtain the final profile models. As for l-alanine and citrinin, a least-squares fit (of the tails only) to a Cauchy function was considered the appropriate procedure for BCA. Fig. 4 shows the final model profile at $2\theta = 95.0^\circ$, superimposed on the background-free 96-step experimental profile of reflection $-16,0,12$, collected at $2\theta = 95.59^\circ$. The excellent agreement of the model profile with the experimental one is clearly evident; in particular, it can be noted that the calculated quantities for steps 1 and 96 are almost exactly coincident with the experimental values.

Table 1. Truncation losses $[100(B+C)/A]$ obtained from the synthetic intensity profiles for four scan ranges

| 2θ (deg.) | 2θ scan ranges ^A | | | |
|---------------------|------------------------------------|---------|---------|---------|
| | $3.4+S$ | $2.5+S$ | $2.0+S$ | $1.5+S$ |
| 5 | — | 0.3 | 1.3 | 2.8 |
| 15 | 0.3 | 1.7 | 2.9 | 4.2 |
| 25 | 1.2 | 2.4 | 3.8 | 5.6 |
| 35 | 2.3 | 4.2 | 5.7 | 8.0 |
| 45 | 3.6 | 5.6 | 7.3 | 9.0 |
| 55 | 4.6 | 6.5 | 8.1 | 10.6 |
| 65 | 6.2 | 7.9 | 9.4 | 11.8 |
| 75 | 7.3 | 9.2 | 10.8 | 13.2 |
| 85 | 8.3 | 10.1 | 11.6 | 14.3 |
| 95 | 9.2 | 11.2 | 13.0 | 15.9 |
| 105 | 10.3 | 13.1 | 15.6 | 19.7 |

^A S is the α_1 - α_2 splitting for Mo radiation.

**Fig. 5.** Truncation losses (see Table 1).**Table 2.** Truncation losses $100B/A$ under the peak for the 2θ scan range $2.5+S$

| 2θ (deg.) | Method 1 ^A | Method 2 ^B |
|------------------|-----------------------|-----------------------|
| 5 | 0.3 | 0.0 |
| 15 | 1.6 | 0.8 |
| 25 | 2.2 | 1.3 |
| 35 | 3.9 | 3.6 |
| 45 | 4.1 | 4.3 |
| 55 | 4.5 | 5.0 |
| 65 | 5.0 | 5.5 |
| 75 | 5.5 | 6.1 |
| 85 | 5.8 | 6.3 |
| 95 | 6.3 | 7.2 |
| 105 | 7.6 | 8.6 |

^A Derived from the synthetic profiles.

^B Obtained by subtracting the inherent background from the experimental background for the 11959 measured intensities of set 1.

A close inspection of the Fourier components of the average aberration functions reveals a well-defined 2θ dependence. Studies on this relationship, including parametrisation of the dependence by a set of analytical functions of 2θ , are in progress.

5. Results

Table 1 gives the truncation losses for four scan ranges in 2θ values, calculated from the final model profiles. As seen from Fig. 5, the losses can be separated into two parts, *B* and *C*: the former, within the scan range, is due to overestimation of the background, the latter to the tailing of the profile beyond the scan limits. The values of the portion under the peak, as derived from the treatment described here, can be compared with those obtained by subtracting the inherent background from the experimental apparent background measured for each reflection during the collection of a given set of data. For the extensive set 1 of BCA the comparison is made in Table 2; values derived from the model profiles appear slightly overestimated at low 2θ values and somewhat underestimated in the high 2θ region, but the largest discrepancy amounts to only 1%, possibly an estimate of the accuracy to which truncation losses can be assessed by this method.

The values reported in Tables 1 and 2, again similar but not identical to those of l-alanine and citrinin, further support the conclusions drawn by DM after analysis of those two crystals: (1) the truncation losses in single-crystal X-ray diffractometry are far larger than previously assumed or predicted; and (2) the corrections calculated by this method must be considered entirely empirical.

References

- Albertsson, J., Oskarsson, Å, and Ståhl, K. (1979). *J. Appl. Cryst.* **12**, 537–44.
Arndt, U. W., and Willis, B. T. M. (1966). In 'Single Crystal Diffractometry', p. 287 (Cambridge Univ. Press).
Coppens, P., Ross, F. K., Blessing, R. H., Cooper, W. F., Larsen, F. K., Leipoldt, J. G., and Rees, B. (1974). *J. Appl. Cryst.* **7**, 315–19.
Denne, W. A. (1977). *Acta Cryst. A* **33**, 438–40.
Destro, R., and Marsh, R. E. (1987). *Acta Cryst. A* **43**, 711–18.
Destro, R., and Simonetta, M. (1977). *Acta Cryst. B* **33**, 3219–21.
Samson, S., Goldish, E., and Dick, C. J. (1980). *J. Appl. Cryst.* **13**, 425–32.